Validation of GLASS albedo product through Landsat TM data and ground measurements

WANG Lizhao[1], ZHENG Xuechang[2], SUN Lin[2], LIU Qiang[1,3], LIU Suhong[1]

1. *State Key Laboratory of Remote Sensing Science, Research Center for Remote Sensing and GIS, and School of Geography, Beijing Normal University, Beijing* 100875, *China*;
2. *College of Geomatics, Shandong University of Science and Technology, Shandong, Qingdao* 266590, *China*;
3. *College of Global Change and Earth System Science, Beijing Normal University, Beijing* 100875, *China*

Abstract: The Global LAnd Surface Satellite Products System (GLASS) albedo product provides a gap-filled shortwave albedo map with high temporal resolution through which the occurrence of snow and rain and the variation of vegetation status can be d etected. The GLASS albedo is retrieved with the Angular Bin (AB) algorithm, which can estimate the shortwave albedo from a single observation of reflectance. To assess the accuracy of this albedo product, FLUXNET observations were used to calculate the actual surface albedo as the true value to validate the high-spatial resolution albedo derived from Landsat Thematic Mapper (TM) imagery at 30 m by the AB algorithm. The Landsat TM albedo was then aggregated to 1 km resolution and was compared with the GLASS albedo at 1 km. The absolute error of the GLASS albedo is less than 0.0163, which demonstrates itsreliabilityfor most a pplication requirements.

Key words: albedo validation, GLASS, TM, scaling, FLUXNET

CLC number: TP79 **Document code:** A

Citation format: **Wang L Z, Zheng X C, Sun L, Liu Q and Liu S H. 2014. Validation of GLASS albedo product through Landsat TM data and ground measurements. Journal of R emote Sensing, 1 8(3): 547 - 558 [DOI: 10.11834/jrs.20143130]**

1 INTRODUCTION

Land surface albedo is the ratio of reflected radiation from the surface to incident radiation, which is determined by the characteristics of the ground surface (Dickinson,1983). Albedo is a critical parameter in surface radiation budget, numerical weather models, and the global climate system. A general agreement onalbedo accuracy for research on these fields is 0.02—0.05 units in absolute albedo value (Sellers, et al., 1995; Mason, et al., 2005).

The shortwave albedo is one of the five long-term land-surface key parameters (LAI, albedo, emissivity, downward shortwave radiation, and PAR) generated by the Global LAnd Surface Satellite product system (GLASS) project. The GLASS shortwave albedo product is derived by the Angular Bin (AB) algorithm and is gap-filled by the Statistics-based Temporal Filtering (STF) algorithm. The accuracy of this new albedo product requires evaluation. The scale mismatch between ground measurements and satellite products cannot be ignored in the validation, especially for coarse-resolution satellite products. The 1 km GLASS albedo product cannot be directly validated by ground measurements unless the ground measurement sites are homogeneous.

There are two validation approaches that aim to reduce the scale effect in the validation. One method assesses the spatial representativeness of the measurement of the site before the validation and assumes that the scale effect at sites with high representativeness can be ignored. Susaki (2007) examined the homogeneity of the site by calculating the semivariance of ASTER & Landsat ETM + imagery around the site.

Another approach uses high-resolution imagery to upscale ground measurements to the coarse-resolution pixel scale. Liang (2002) used ETM + imagery to upscale ground measurements to the MODIS pixel scale and validated the MODIS albedo product throughthe measurements at Beltsville. The Lambert assumption in the retrieval of ETM + albedo may affect the accuracy of the validation. Jiao (2005) validated MODIS albedo with field measurements upscaled through airborne data.

The validation approach used in this study is the second one. Landsat Thematic Mapper (TM) albedo is used as the high-resolution albedoand is retrieved through the AB algorithm. TM albedo is the bridge to upscaleground measurements to 1 km resolution and then to validate GLASS albedo. This validation method is summarized as "one test and two matches" by Zhang,

Received: 2013-05-22; **Accepted:** 2013-09-28; **Version of record first published:** 2013-10-05

Foundation: National High Technology Research and Development Program of China (863 Program) (No. 2009AA122100); National Natural Science Foundation of China (No. 41171262)

First author biography: WANG Lizhao (1986—), male, master candidate, he majors in quantitative remote sensing. E-mail:wlz1220@sina.com

Corresponding author biography: LIU Qiang (1974—), male, associate professor. His research interest is remote sensing applications. E-mail:toliuqiang@bnu.edu.cn

et al. (2010).

2 DATASETS

2.1 FLUXNET datasets

FLUXNET is a global network of micrometeorological tower sites that use eddy covariance methods to measure the e xchanges of carbon dioxide, water vapor, and energy between the biosphere and atmosphere ([2013-11-15] http://fluxnet. ornl. gov/). Many of these sites collect shortwave radiation fluxes, which can be used to calculate surface albedo. Five FLUXNET sites covered with grass and Deciduous Broad-leaved Forest (DBF), are used in this validation. These sites are distributed in north America and Asia.

Table 1 FLUXNET sites in validation

Site name	Latitude	Longitude	Land cover type	Time range	Number of TM images
KBU	47.2140°N	-108.7373°E	Grass	2003—2008	17
Kendall_Grassland	31.7365°N	109.9420°W	Grass	2004—2007	52
Morgan	39.3231°N	86.4131°W	DBF	1999—2007	12
Walker_Branch	35.9588°N	84.2874°W	DBF	2001—2007	60
Willow_Creek	45.8059°N	90.0799°W	DBF	1998—2006	62

2.2 GLASS albedo product

The GLASS albedo product is available from 1985 to 2010. This productis derived from different data sources before and after 2000. The product from 1985 to 2000 is derived from AVHRR data generated by the Long-Term Land Data Record (LTDR) project. The final product is composed of data in a 3 2-day temporal window and has a spatial resolution of 0.05° and a temporal step of eight days. The product after 2000 is d erived from MODIS directional reflectance. The final product is composed of data in a 16 day temporal window and has a spatial resolution of 1 km and a temporal step of one day.

GLASS albedo is retrievedby the AB algorithm, which builds a linear regression relationship between the ground-surface directional reflectance and broadband albedo at local noon. The GLASS albedo product is derived from one single-directional reflectance imagery and can thus detect the rapid changes of land surface, such as snow, rain and vegetation growth.

Two branches in the AB algorithm are applicable to different circumstances. The branch that requiresthe input of s urface directional reflectance is called AB1, and the other that requires the input of top-of-atmosphere directional reflectance is called AB2. Given that MODIS sensors are carried by Terra and Aqua, four intermediate products are generated by AB1 and AB2. To fill the gaps in these intermediate products and generate a merged product based on them, an STF algorithm is developed. The final GLASS albedo product, gap-filled land-surface shortwave Black-Sky Albedo (BSA) and White-Sky Albedo (WSA) with aquality control flag, is produced.

2.3 TM images

TM imagery with seven bands (three in visible wavelengths, four in infrared) is introduced in this research as the upscaling bridge. The TM sensors are carried by Landsat satellites. The i mage data can be downloaded at the website of USGS ([2013-11-15] http://edcsns17. cr. usgs. gov/EarthExplorer/). A total of 203 TM images of the five FLUXNET sites are collected.

3 METHOD

3.1 TM albedo retrieval

To estimate the land surface albedo, Liang (2002) assumed the surface to be Lambertian and used narrowband-t o-broadband albedo conversions to produce land surface albedo. In this paper, AB algorithm is used to calculate broadband TM albedo because it empirically corrects the anisotropy of the land surface. Furthermore, Zhang(2010) proposed the algorithm of the high- and coarse-resolution albedo to be the same.

TM imagery albedo is retrieved below. (1) The solar/view geometry space is divided into several angular bins. (2) Measurements in the POLDER-3/PARASOL BRDF dataset are transferred to be consistent in wavelengths with TM data. (3) A ccording to the BRDF information in the training dataset, n arrowband albedo is derived throughthe linear kernel-driven model. The broadband albedo is then calculated by narrowband-to-broadband conversion relationships (Liang, 2002). (4) An e mpirical relationship between directional reflectance and broadband albedo for each angular bin in the first step is developed. (5) According to the solar and view geometry of the TM imagery, the relationship between the TM reflectance and broadband albedo is retrieved.

Given that the TM sensor observes the surface from a nadir view, the view zenith and azimuth angles are set to zero in inversion. The solar zenith and azimuth angles can be extracted from the metadata (MTL files) of the TM images.

3.2 Comparison of ground measurements and TM albedo

The records ofthe FLUXNET sites include the upward and downward shortwave radiation flux atan interval of 30 min. The upward and downward radiation within 1 h around the local noon is averaged to reduce the fluctuation caused by clouds, and the ratio of the averaged upward radiation (Rg_out) to the averaged downward radiation (Rg) is the albedo at noon.

$$\alpha\_site = (Rg\_out)/Rg \quad (1)$$

The BSA and WSA albedos are retrieved from the TM i

mages by the AB algorithm. These albedosare composed into blue-sky albedo with Eq. (2) (Lewis & Barnsley, 1994).

$$\alpha\_actual = \alpha\_bs \cdot (1 - r\_d) + \alpha\_ws \cdot r\_d \quad (2)$$

$$r\_d = 0.122 + 0.85\exp(-4.8 \cdot \mu_0) \quad (3)$$

where α_actual, α_bs, and α_ws denote the blue-sky, black-sky, and white-sky albedos, respectively. r_d is the fraction of the d iffuse radiation. μ_0 is the cosine of SZA at local noon.

Considering that 80% of measured radiations are c ontributed from a circular area of 10 m to 20 m (Cescatti, e t al., 2012), the scale of ground measurements is close to that of a TM pixel. To lessen the influence of geometric mismatc-hing, the average value of TM albedo in a 3 × 3 window is used in the validation.

3.3 Comparison of TM albedo and GLASS albedo

TM albedo is used as the bridge in the upscaling of ground measurements to the scale of a GLASS pixel. According to Liang's simulation (Liang,et al., 2002), the aggregation from 3 0 m albedo to 1 km albedo is linear in flat areas. The TM albedo is validated with ground measurements and is then averaged in a 3 3 × 33 window (an approximately 1 km × 1 km area) centered at the collocated GLASS pixel to be the reference value of the GLASS albedo.

To eliminate the geometric mismatching between the TM al-bedo and GLASS albedo, the average TM albedo in a 165 × 165 window is compared with the average GLASS albedo in a 5 × 5 window (an approximately 5 km × 5 km area).

4 RESULT AND DISCUSSION

4.1 Ground measurements and TM albedo

A total of 103 cloud-free TM images cover the five selected FLUXNET sites. The validation results of the TM albedo with the ground measurements are shown in Fig. 1 and Table 2. The total RMSE and determination coefficient are 0.0172 and 0.9132, re-spectively.

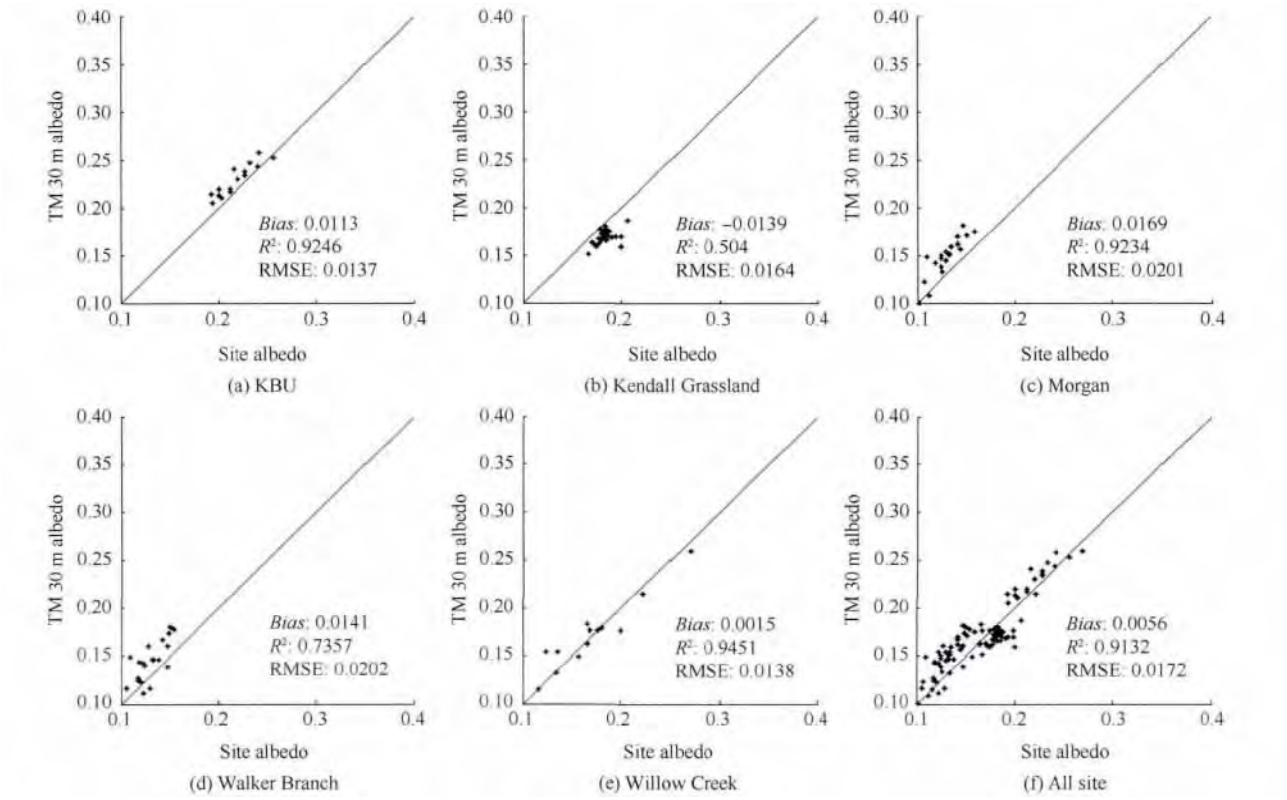

Fig. 1 Comparison between ground measurements and TM albedo

Table 2 Result of validation of TM albedo

Index	KBU	Kendall	Morgan	Walker	Willow	Total
Bias	0.0113	−0.0139	0.0169	0.0141	0.0015	0.0056
RMSE	0.0137	0.0164	0.0201	0.0202	0.0138	0.0172
R^2	0.9246	0.5040	0.9234	0.7357	0.9451	0.9132

The validation result shows the desiredconsistency of the ground measurements and the TM albedo, except that the deter-mination coefficient at Kendall is low (0.504). The reason is that the range of albedo values at Kendall is relatively narrow (0.15—0.20). The determination coefficients at other sites are higher than 0.7.

4.2 TM albedo and GLASS albedo

The aggregated TM albedo is compared with the GLASS a lbedo at two spatial scales (1 km × 1 km and 5 km × 5 km). The RMSE between their valid and cloud-free records is 0.0121 (1 km × 1 km) and 0.0124 (5 km × 5 km). The results are shown in Fig. 2 and Table 3.

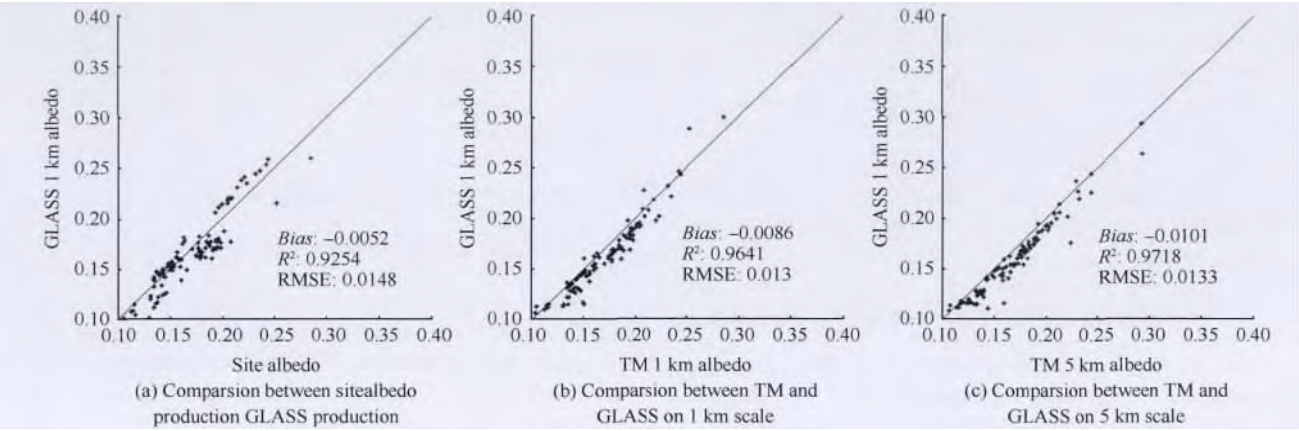

Fig. 2 Scatter plot of GLASS albedo validation

Table 3 Result of validation of GLASS albedo

Index	Directcomparison	1 km scalecomparison	5 km scalecomparison
Bias	−0.0052	−0.0086	−0.0101
R^2	0.9254	0.9641	0.9718
RMSE	0.0148	0.0130	0.0133

The validation results illustrate that the consistency of the TM albedo and GLASS albedo is high. The RMSE between the ground measurements and GLASS albedo is larger than the that-between the TM albedo and GLASS albedo because of the scale effect between ground measurements and GLASS albedo. The RMSE and determination coefficients between the TM albedo and GLASS albedo at two different scales are both around 0.13 and 0.96, respectively. The scatter points of the direct comparison between the ground measurements and GLASS albedo are evenly distributed around the Y = X line, whereasthose of the comparison between the TM albedo and GLASS albedo focus on one side becausethe aggregated TM albedo isapparently higher than the GLASS albedo. The deviation at the 5 km scale is greater than that at the 1km scale. This deviation may be caused by the systematic error in aggregation and can be identified by more validation work. Comparedwiththe direct validation result, the validation result with TM aggregated albedo has high determination coefficient and correlation.

4.3 Total accuracy and influence factors

The discrepancy between ground measurements and TM a lbedo and between TM albedo and GLASS albedo is listed a bove. With the assumption ofthe scale effect between albedo at 30 m and that at 1 km, the squared error between the 1 km ground measured albedo and the GLASS albedo does not exceed the sum of the two squared errors, indicating that theRMSE of the 1km ground measured albedo and GLASS albedo does not exceed 0.163. This accuracy demonstrates that the GLASS albedo product satisfies the application requirement.

Generally, the actual error cannot reach the upper bound b ecause the unbiased random errors usually cancel each other out, but the bias error is reserved. Thus,an unbiased algorithm for retrieving high-resolution albedo is an important condition. The comparison between ground measurements and TM albedo reveals a non-significant bias. However, this study does not e xamine the error in upscaling further limited by the amount of data and the complexity and difficulty of the research.

Clouds strongly affect validation accuracy. Clouds increase albedo because of their high reflectance; at the same time, the shadow of clouds decreases albedo. To reduce these interferences, only cloud-free data are used in the validation. However, several thin clouds are left in the 1 km × 1 km and 5 km × 5 km areas and cannot be ignored. Another factor that i nfluences the validation result is the heterogeneity of the measurement site; this factor causes scaling error. In this study, several relatively homogeneous measurement sites are chosen to reduce the scaling error. Moreover, the points with high discrepancy are mostly observed in snow. The high reflectance of snow cover i ncreases the absolute error of the albedo but keeps the same r elative error.

5 CONCLUSION

In this study, GLASS albedo is validated with FLUXNET measurements and TM albedo. The AB algorithm used to retrieve TM albedo shows the following advantages. (1) Thenon-Lambertian characteristics of land surface are considered and modified. (2) The algorithmproduces albedo datasets with high temporal resolution. (3) The algorithm contains anatmospheric correction module. However, the AB algorithm is developed only for low-resolution satellite data, and its training dataset isselected from POLDER-BRDF, whose spatial resolution is 6 km. The scale mismatch may cause the instability of the retrieval of TM albedo.

The upscaling method of TM albedo is simplyto averagewithin a GLASS pixel. The terrain effect is disregarded, which may increase error in the validation result. In the comparison b

etween the TM albedo and GLASS albedo, the positive bias between them shows that some systematic error may have been introduced in the validation process and thusneeds to further explorationand analysis.

The following conclusions can be drawn from this study.

(1) The TM albedo retrieved by the AB algorithm is validated with FLUXNET observations and shows high accuracy.

(2) The GLASS albedo product can accurately reflect and predict the variation of surface albedo.

Acknowledgements: The ground measurements were freely offered by FLUXNET. The TM images were freely downloaded from the website of the US Geological Survey. The GLASS albedo was kindlyoffered by the GLASS group.

REFERENCES

Cescatti A, Marcolla B, Vannan S K S, Pan J Y, Román M O, Yang X Y, Ciais P, Cook R B, Law B E, Matteucci G, Migliavacca M, Moors E, Richardson A D, Seufert G and Schaaf C B. 2012. Intercomparison of MODIS albedo retrievals and in situ measurements across the global FLUXNET network. Remote Sensing of Environment, 121: 323 – 334 [DOI: 10.1016/j.rse.2012.02.019]

Dickinson R E. 1983. Land surface processes and climate—Surface albedos and energy balance. Advances in Geophysics, 25: 305 – 353

Jiao Z T, Wang J D, Xie L O, Zhang H, Yan G J, He L M and Li X W. 2005. Initial validation of MODIS albedo product by using field measurements and airborne multiangular remote sensing observations. Journal of Remote Sensing, 9(1): 64 – 72

Lewis P and Barnsley M J. 1994. Influence of the sky radiance distribution on various formulations of the earth surface albedo // Proceedings of the Colloque International Mesures Physiques et Signatures en Teledetection. Val d'Isere: France: 707 – 716

Liang S L, Fang H L, Chen M Z, Shuey C J, Walthall C, Daughtry C, Morisette J, Schaaf C and Strahler A. 2002. Validating MODIS land surface reflectance and albedo products: methods and preliminary results. Remote Sensing of Environment, 83(1 – 2): 149 – 162 [DOI: 10.1016/S0034 – 4257(02)00092 – 5]

Liang S L, Stroeve J and Box J E. 2005. Mapping daily snow/ice shortwave broadband albedo from Moderate Resolution Imaging Spectroradiometer (MODIS): the improved direct retrieval algorithm and validation with Greenland in situ measurement. Journal of Geophysical Research: Atmospheres, 110 (D10) [DOI: 10.1029/2004JD005493]

Liu N F, Liu Q, Wang L Z and Wen J G. 2011. A temporal filtering algorithm to reconstruct daily albedo series based on GLASS albedo product // Proceedings of the 2011 IEEE International Geoscience and Remote Sensing Symposium. Vancouver, BC: IEEE: 4227 – 4280 [DOI: 10.1109/IGARSS.2011.6050176]

Mason P. 2005. Implementation plan for the global observing system for climate in support of the UNFCCC. 21st International Conference on Interactive Information Processing Systems (IIPS) for Meteorology, Oceanography, and Hydrology. San Diego, CA, USA.

Qu Y, Liu Q, Liang S, Wang L, Liu N and Liu S. 2012. Direct-estimation algorithm for mapping daily land-surface broadband albedo from MODIS data. IEEE Transactions on Geoscience and Remote Sensing, PP(99): 1 [DOI: 10.1109/TGRS.2013.2245670]

Román M O, Schaaf C B, Woodcock C E, Strahler A H, Yang X Y, Braswell R H, Curtis P S, Davis K J, Dragoni D, Goulden M L, Gu L H, Hollinger D Y, Kolb T E, Meyers T P, Munger J W, Privette J L, Richardson A D, Wilson T B and Wofsy S C. 2009. The MODIS (Collection V005) BRDF/albedo product: assessment of spatial representativeness over forested landscapes. Remote Sensing of Environment, 113(11): 2476 – 2498 [DOI: 10.1016/j.rse.2009.07.009]

Sellers P J, Meeson B W, Hall F G, Asrar G, Murphy R E, Schiffer R A, Bretherton F P, Dickinson R E, Ellingson R G, Field C B, Huemmrich K F, Justice C O, Melack J M, Roulet N T, Schimel D S and Try P D. 1995. Remote sensing of the land surface for studies of global change: Models—algorithms—experiments. Remote Sensing of Environment, 51(1): 3 – 26 [DOI: 10.1016/0034 – 4257(94)00061 – Q]

Stokes G M and Schwartz S E. 1994. The Atmospheric Radiation Measurement (ARM) Program: programmatic background and design of the cloud and radiation test bed. Bulletin of the American Meteorological Society, 75(7): 1201 – 1221 [DOI: 10.1175/1520 – 0477(1994)075 < 1201:TARMPP > 2.0.CO;2]

Susaki J, Yasuoka Y, Kajiwara K, Honda Y and Hara K. 2007. Validation of MODIS albedo products of paddy fields in Japan. IEEE Transactions on Geoscience and Remote Sensing, 45(1): 206 – 217 [DOI: 10.1109/TGRS.2006.882266]

Zhang R H, Tian J, Li Z L, Su H B, Chen S H and Tang X Z. 2010. Principles and methods for the validation of quantitative remote sensing products. Science China Earth Sciences, 53(5): 741 – 751 [DOI: 10.1007/s11430 – 010 – 0021 – 3]

利用 Landsat TM 数据和地面观测数据验证 GLASS 反照率产品

王立钊[1]，郑学昌[2]，孙林[2]，刘强[1,3]，刘素红[1]

1. 北京师范大学遥感科学国家重点实验室，遥感与地理信息系统研究中心，地理学与遥感科学学院，北京 100875；
2. 山东科技大学测绘学院，山东 青岛 266590；
3. 北京师范大学 全球变化与地球系统科学研究院，北京 100875

摘 要：Global LAnd Surface Satellite Products System(GLASS)反照率产品基于 Angular Bin(AB)算法，仅使用单一观测角度的地表或大气层顶反射率数据就能较为准确地反演地表宽波段反照率，具有较高的时间分辨率，可以反映降雪、融雪、收割等状况下地表反照率的快速变化。遵循“一检两恰”的验证流程对这一反照率产品进行验证，首先使用 FLUXNET 站点验证数据对 AB 算法反演的 Landsat Thematic Mapper (TM)高分辨地表反照率数据进行验证，再将 TM 高分辨反照率聚合到 GLASS 像元尺度对 GLASS 反照率产品进行验证。挑选 FLUXNET 的 5 个站点，筛选无云条件下的 TM 高分辨率影像，共获得 103 组有效验证数据。验证结果表明，GLASS 反照率产品具有较高的精度，总体误差约为 0.0163，可以满足大多数应用的精度需求。

关键词：反照率验证，GLASS，TM，尺度转换，FLUXNET

中图分类号：TP79 **文献标志码**：A

引用格式：王立钊，郑学昌，孙林，刘强，刘素红. 2014. 利用 Landsat TM 数据和地面观测数据验证 GLASS 反照率产品. 遥感学报，18(3)：547－558

Wang L Z, Zheng X C, Sun L, Liu Q and Liu S H. 2014. Validation of GLASS albedo product through Landsat TM data and ground measurements. Journal of R emote Sensing, 1 8(3): 547－558 [DOI: 10.11834/jrs.20143130]

1 引 言

地表反照率反映了陆地表面对太阳辐射的反射能力，其定义为太阳辐射短波波段在半球空间的所有地表反射辐射与所有入射能量之比(Dickinson，1983)。地表反照率在地表能量平衡、天气预报参数化、气象监测和气候影响评价、陆地系统中土壤和植被建模等研究中具有重要意义，是地表辐射平衡和全球气候系统研究中的重要参数(Mason，2005)。这些应用对反照率的精度要求一般为 0.02—0.05(Sellers 等，1995)。

地表宽波段反照率产品是全球陆表特征参量产品生成与应用研究系统 GLASS(Global LAnd Surface Satellite products system)生产的 5 种陆表特征参量(叶面积指数、地表反照率、发射率、下行短波辐射、下行光合有效辐射)之一。GLASS 反照率产品采用了直接反演算法(Liang 等，2005；Qu 等，2012)与时空滤波算法(Liu，2011)配合使用的方式，得到无缺失的全球陆表反照率数据集。新算法反演的 GLASS 反照率产品，需要大量的验证工作以对其产品精度进行评价。

在使用地面实测数据验证卫星产品时，站点数据与卫星产品间的尺度差异是必须考虑的问题(Liang 等，2002)。特别是对于 GLASS 分辨率为 1 km 的反照率产品，除非像元内地表覆盖非常均一，否则无法以地面测量的点数据代表像元的面数据，即不

收稿日期：2013-05-22；修订日期：2013-09-28；优先数字出版日期：2013-10-05

基金项目：国家高技术研究发展计划(863 计划)(编号：2009AA122100)；国家自然科学基金(编号：41171262)

第一作者简介：王立钊(1986—)，男，硕士研究生，主要研究方向为定量遥感，高光谱遥感等方面的研究，已发表论文 2 篇。E-mail：wlz1220@sina.com

通信作者简介：刘强(1974—)，男，副教授，博士生导师。主要从事定量遥感中的多角度遥感、二向反射、反照率和热红外辐射方向性等研究，特别是在多角度遥感数据的获取、处理、建模与反演等方面具有丰富经验，近期致力于开发全球长时间序列地表反照率产品生产算法。E-mail：toliuqiang@bnu.edu.cn

能用站点实测数据直接验证 GLASS 像元尺度的反照率产品。

目前,为解决反照率验证工作中的尺度差异问题,大体有两种研究思路,一种思路是对验证站点依据均一性进行筛选后直接用地面站点观测反照率验证卫星产品。如:Susaki 等人(2007 年)使用 ASTER & Landsat ETM + 的半方差评价验证站点周围的均一性。Roman 等人(2009)提出一系列基于半方差的统计量作为评价站点均匀性的指标。对通过均一性检验的站点,可以直接使用地面测量值验证 MODIS 反照率产品。

另一种思路是通过高分辨率遥感数据对地面站点验证数据进行升尺度转换后再用来验证低分辨率遥感产品。Liang 等人(2002)用美国农业部在 Beltsville 的观测数据对 MODIS(250—1000 m)产品进行验证,其中使用了 ETM + 数据进行升尺度。但是由于 ETM + 数据缺少多角度信息,而只能采用地表朗伯假设反演 ETM + 的反照率,精度受到影响。焦子锑等人(2005)使用机载 AMTIS 多角度遥感数据来进行尺度转换,验证 MODIS 反照率数据。但 MODIS 反照率产品是基于 16 天内累积观测的多角度反射率反演所得,地面站点数据则是对 1 天内地表反照率的观测,两者在时间上的不匹配会影响验证的精度。

本文在第 2 种思路的基础上,基于 Angular Bin (AB)算法对 Landsat Thematic Mapper (TM)数据的反照率反演算法进行了改进,通过地面验证站点数据对 TM 反照率反演精度进行评价,再利用升尺度后的 TM 反照率数据评价 GLASS 反照率产品,实现了“一检两恰”(Zhang 等, 2010)的验证流程。

2 数 据

2.1 FLUXNET 数据集

FLUXNET 是一个以全世界广泛分布的通量塔为基础的全球通量观测网络([2013-11-15] http://fluxnet.ornl.gov/),负责收集、存档、发布从世界各地的通量塔观测的二氧化碳、水汽、能量等通量数据。其中许多站点提供上行短波辐射通量和下行短波辐射通量的观测值,用上行短波辐射通量除以下行短波辐射通量,可计算站点的地表反照率,用以验证卫星反照率产品。

本文共选择 5 个 FLUXNET 站点(表 1)的数据进行验证。这些站点分布在北美洲和亚洲,地表覆盖类型包括草地和落叶阔叶林地。

表 1 FLUXNET 验证站点信息表

站点名	纬度	经度	覆盖类型	位置	时间范围/年	TM 下载数量
KBU	47.2140°N	108.7373°E	草地	蒙古	2003—2008	17
Kendall_Grassland	31.7365°N	109.9420°W	草地	美国亚利桑那州	2004—2007	52
Morgan	39.3231°N	86.4131°W	落叶阔叶林	美国印第安纳州	1999—2007	12
Walker_Branch	35.9588°N	84.2874°W	落叶阔叶林	美国田纳西州	2001—2007	60
Willow_Creek	45.8059°N	90.0799°W	落叶阔叶林	美国威斯康星州	1998—2006	62

2.2 GLASS 反照率产品

GLASS 反照率产品生产 1985 年—2010 年地表反照率数据。1985 年—1999 年基于 AHVRR 数据生产的地表反照率数据空间分辨率 0.05°,合成时间窗口为 32 天,合成间隔 8 天;2000 年—2010 年基于 MODIS 数据生产的地表反照率数据空间分辨率 1 km,合成时间窗口为 16 天,合成间隔 1 天。本文重点对基于 MODIS 反射率数据生产的 GLASS 反照率产品进行验证。该数据包括短波(0.3—5.0 μm)黑空反照率、白空反照率以及质量控制数据(QC)。GLASS 反照率产品基于 AB 算法对 MODIS 地表(或大气层顶)反射率数据进行反演,AB 算法通过建立地表(或大气层顶)二向反射率与地表宽波段反照率之间的统计关系对宽波段反照率的反演。为了考虑地表的二向反射特性,AB 算法将太阳天顶角、观测天顶角和相对方位角组成的角度空间划分为若干网格,在不同网格上使用不同的经验关系。因为只使用单一观测角度的地表或大气层顶反射率数据就能较为准确地反演出地表宽波段反照率,AB 算法有较高的时间分辨率,可以反映出降雪、融雪、农作物收割等地表反照率快速变化的过程。

因为 EOS 计划中的 Terra 和 Aqua 卫星都搭载 MODIS 传感器,分别获得上午和下午的观测数据,

而 AB 算法又分为使用大气校正的地表反射率和直接使用大气层顶反射率两种工作模式,因此 AB 算法的输出是 4 种初级产品。这些初级产品之中会有很多空缺,这是由原始数据的缺失或者云的覆盖引起的,另外,AB 算法虽然对地表非朗伯性有所考虑,但是仍然受到数据噪声或者大气校正残余误差的影响,时间序列抖动比较大。因此 GLASS 系统并不直接向用户发布初步产品(即 AB 算法的结果),而是使用基于统计知识的时间序列滤波 STF(Statistics-based Temporal Filtering)算法对初级产品进行合成和滤波,并填补空缺(Liu 等,2011),得到最终产品。STF 算法基于贝叶斯统计学原理,利用从美国 NASA 发布的 MODIS 标准产品(MCD43B3)统计出全球不同地区地表反照率的均值、标准差和时间序列自相关性,作为先验知识库用于支持 4 种反照率初级产品的后处理。

2.3 TM 高分辨影像数据

本文中使用 TM 高分辨率影像作为地面站点和 GLASS 像元之间尺度转换的桥梁。TM 是搭载在 Landsat 系列卫星上的主要传感器之一,共有 7 个波段,分布在短波和热红外波段上,其中短波波段部分的空间分辨率为 30 m,热红外部分分辨率为 120 m。美国国家地质勘探局(USGS)的([2013-11-15] http://earthexplorer.usgs.gov/)网站提供了 TM、ETM+图像数据的免费下载。根据验证需求,共收集覆盖 5 个 FLUXNET 站点共 203 幅 TM 影像数据。

3 方 法

3.1 TM 高分辨反照率反演

使用 TM 这类单一观测角度的遥感数据计算反照率时,往往简单认为垂直观测的波段反射率就是该波段的反照率,直接进行窄波段反照率向宽波段反照率的转换。因为忽略了地表的非朗伯性,往往精度较低。GLASS 系统中用于反演 MODIS 数据的 AB 算法可以在单一观测角度的条件下考虑地表二向反射特性的校正,克服了简单算法的不足(Qu 等,2012)。另外,根据 Zhang 等人(2010)的研究,在对低分辨率像元尺度遥感产品的验证中,“一捡两恰”需要用相同的遥感模型同时反演高分辨率与低分辨率的遥感参数,因此本文使用针对 TM 数据的 AB 算法计算 TM 高分辨率的地表反照率产品。

对 TM 数据进行的预处理主要是几何精校正和辐射定标两方面。几何精校正通过人工目视选取地面控制点的方式进行,辐射定标利用了 TM 数据元数据中提供的定标系数。对大气影响的考虑是由集成在 AB 算法中的大气辐射传输模块完成(Qu 等,2012),所以在预处理过程中,不对 TM 影像进行大气纠正。

用于 TM 数据的 AB 算法流程为:

步骤 1 将太阳天顶角、观测天顶角和相对方位角组成的角度空间划分为若干网格。

步骤 2 基于 POLDER-3/PARASOL BRDF 数据集中的地表方向反射率数据,经过筛选和插值以及波段转换得到模拟的 TM 反射率数据(如从大气层顶反射率反演,则需进行大气辐射传输的模拟过程)。

步骤 3 对 POLDER-3/PARASOL BRDF 数据集中的地表方向波谱反射率采用改进的线性核驱动模型(模拟冰雪反射特性,增加前向散射核)(Qu 等,2012)进行半球积分获得 POLDER 窄波段反照率,并将波段转换为 TM 窄波段反照率,再通过窄波段向宽波段反照率转换公式模拟地表宽波段反照率。因为 AB 算法中的 BRDF 信息来自 POLDER 多角度观测数据集,而 POLDER 传感器只有可见光近红外波段,所以 AB 算法只使用了可见光近红外的 4 个波段。

步骤 4 按照步骤 1 中划分的网格空间中的各个格网分别建立 TM 方向反射率和地表宽波段反照率间的回归关系,将其存储为查找表。

步骤 5 根据从 TM 方向反射率产品中读取的反射率及角度等信息,检索查找表并插值获得相应的回归关系,反演出地表宽波段反照率数据。

由于 TM 传感器为从天顶方向垂直向下观测,为简化反演过程,其中观测天顶角和观测方位角近似为 0°,太阳天顶角和方位角可以从 TM 的元数据 MTL 文件中读取。

3.2 站点地表反照率与 TM 反演反照率比较

待验证的 FLUXNET 站点数据中观测了半小时间隔的上行和下行短波辐射通量数据。站点地表反照率计算过程中,先将当地时刻接近正午的 2 小时内(±1 小时)的上行和下行短波辐射数据分别平均以减弱云干扰给正午时刻观测数据带来的误差(Román 等,2009),再以平均后的上行辐射(Rg_out)与下行辐射(Rg)间的比值作为站点地表反照率数据。

$$\alpha\_site = (Rg\_out)/Rg \quad (1)$$

TM 影像经 AB 算法反演后获得短波黑空和白空反照率，但为了和地面测量的地表反照率数据相比较，需进一步计算地表真实反照率。地表真实反照率由黑空反照率和白空反照率按天空散射比因子线性加权计算获得（Lewis 和 Barnsley，1994）。因为本文所选用的 TM 数据均是晴空条件下获得的，所以天空散射比因子可以由晴空条件的经验统计关系获得（Stokes 和 Schwartz，1994）。

$$\alpha\_actual = \alpha\_bs \cdot (1 - r\_d) + \alpha\_ws \cdot r\_d \quad (2)$$

$$r\_d = 0.122 + 0.85\exp(-4.8 \cdot \mu_0) \quad (3)$$

式中，α_actual，α_bs，α_ws 分别指真实反照率、黑空反照率和白空反照率，r_d 为天空散射比因子，μ_0 是太阳天顶角的余弦值。

FLUXNET 站点观测的反照率数据，其观测信号约 80% 的能量来自通量塔周围 10—20 m 内（Cescatti等，2012），与 TM 数据分辨率尺度接近。为了减小几何配准误差造成的影响，验证时 TM 反照率值取 3×3 窗口内像元反照率的平均值。

3.3 TM 聚合反照率与 GLASS 反照率比较

TM 反演反照率是地面站点观测反照率升尺度到 GLASS 像元尺度的桥梁。在用地面站点反照率验证 TM 反照率后，将 TM 反照率聚合到 GLASS 像元大小。以验证站点所对应的 GLASS 像元中心为窗口中心，对 33 像元×33 像元窗口（约为 1 km×1 km范围）内像元进行聚合。在平坦地形条件下从 30 m 像元反射率或反照率到 1000 m 像元尺度的聚合是线性的，直接进行平均的误差可以忽略（Liang 等，2002）。因此，聚合时对窗口内 3 3×33 个像元的反照率进行平均，以其平均值作为聚合后像元的反照率值。按照式（2）（3）计算 TM 聚合影像和 GLASS 产品的真实反照率，并进行对比验证。

为减小 MODIS 像元几何定位不确定性造成的影响，将对 TM 反照率的聚合窗口扩大到 165×165，对 GLASS 反照率像元按 5×5 窗口（5 km×5 km 范围）进行聚合。计算聚合后的真实反照率，并进行比较验证。

4 结果与讨论

4.1 站点反照率与 TM 反演反照率验证结果

对选定的 5 个 FLUXNET 站点中的反照率验证数据，按照影像时间与站点位置匹配对应的 TM 高分辨率反照率并进行对比验证。剔除掉其中数据缺失和受云干扰的数据，共得到 103 组有效验证数据。这些数据的均方根误差 RMSE 为 0.0172，总决定系数 R^2 为 0.9132。各个站点分别比较验证结果如图 1，统计结果见表 2。

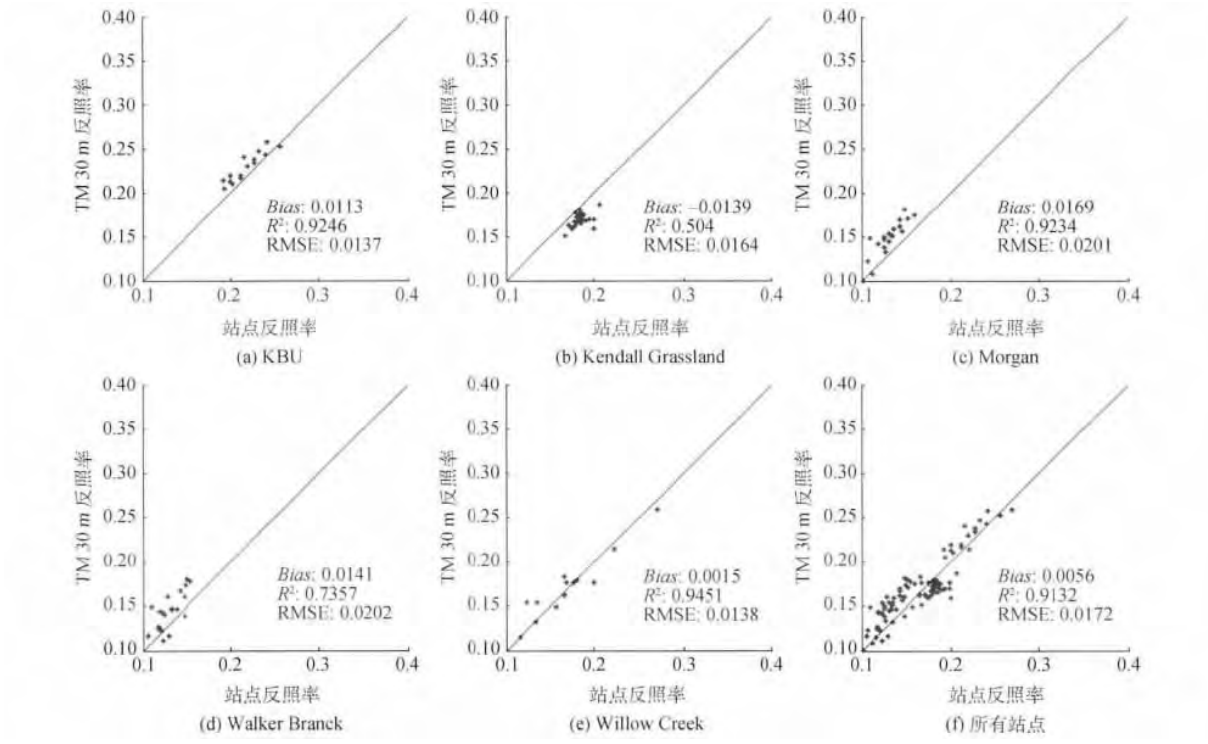

图 1 FLUXNET 站点反照率验证 TM 30 m 反照率散点图

表 2 TM 高分辨率反照率验证结果统计

站点名	KBU	Kendall	Morgan	Walker	Willow	总体
Bias	0.0113	-0.0139	0.0169	0.0141	0.0015	0.0056
RMSE	0.0137	0.0164	0.0201	0.0202	0.0138	0.0172
R^2	0.9246	0.5040	0.9234	0.7357	0.9451	0.9132

验证结果显示,TM 反照率反演结果与地面站点测量数据有较高的一致性。除 Kendall 站点外,其余站点数据和 TM 30 m 反照率间决定系数较大,具有良好的相关性。Kendall 站点的决定系数为 0.504,相对较低,这是由于该站点的反照率值变化范围集中在 0.15—0.20,散点图中的散点分布密集,降低了数据间的相关性。

4.2 TM 反照率与 GLASS 反照率验证结果

对 1 km×1 km 及 5 km×5 km 两种尺度聚合的 TM 反照率和 GLASS 反照率按时间空间匹配并进行比较验证。去除掉其中无效缺失值及受云干扰的记录后,总体 RMSE 分别为 0.0121(1 km×1 km),0.0124(5 km×5 km)。并对地面站点直接验证 GLASS 反照率结果以及 1 km、5 km 两种像元尺度反照率验证结果进行了比较(图 2,统计结果见表 3)。

从验证的统计结果(表 3)来看,3 种验证方式的验证结果都较好。但是直接对地面验证数据和 GLASS 像元反照率之间的比较的 RMSE 明显大于通过 TM 进行过尺度转换的验证结果。1 km 和 5 km两种尺度转换后的验证结果差异很小,RMSE 均在 0.13 左右,R^2 都大于 0.96。从验证的散点图(图 3)分析,直接验证的散点图基本均匀分布在 Y = X 轴两侧,偏差较小。而聚合后验证的反照率则多分布在轴的一侧,TM 聚合反照率明显偏高于待验证的 GLASS 反照率产品,并且 5 km 尺度验证的偏差大于 1 km 尺度的偏差,这可能是聚合过程中的系统误差引起的,但需要对更丰富的验证数据进行比较才能确定。相较于直接验证的结果,TM 聚合反照率的验证的决定系数较高,数据相关性更好。

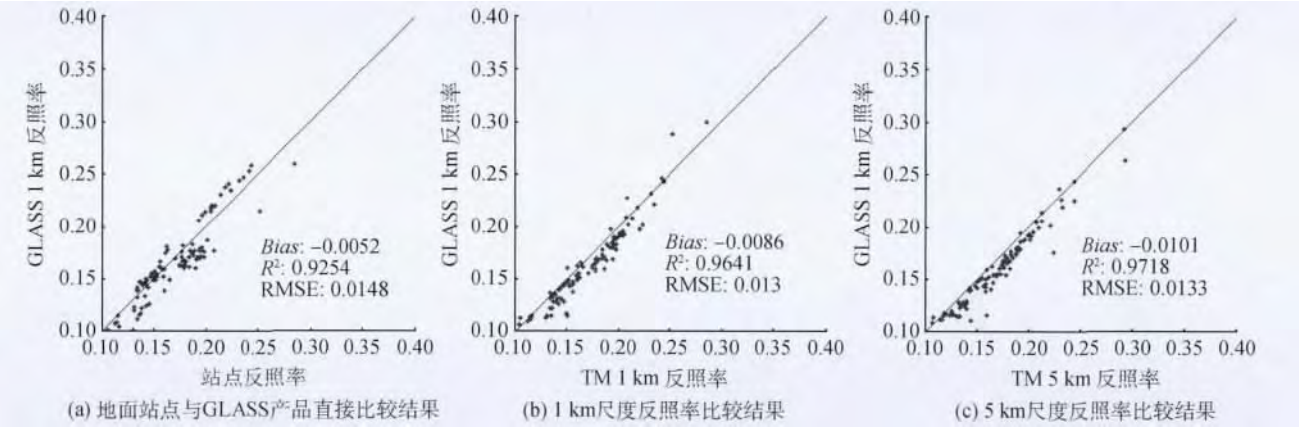

图 2 GLASS 反照率产品验证散点图

表 3 TM 聚合反照率验证 GLASS 反照率结果统计

验证类型	直接比较	1 km 尺度比较	5 km 尺度比较
Bias	-0.0052	-0.0086	-0.0101
R^2	0.9254	0.9641	0.9718
RMSE	0.0148	0.0130	0.0133

4.3 总体误差及其影响因素

前面给出了地面站点与 TM 反照率对比的误差以及 TM 反照率与 GLASS 反照率对比的误差,在 30 m 到 1 km 尺度范围内反照率的尺度效应可以忽略的假设下,根据误差传播理论,像元尺度的地面反照率与 GLASS 产品对比的误差平方的上限应该

不超过上述两个误差的平方和,即 RMSE 大致不超过 0.163,这证明 GLASS 反照率产品已经能够满足应用需求。

一般来说,实际误差并不能达到误差上限,在升尺度变换的聚合过程中,无偏的随机误差常常会相互抵消,而总体偏差(即 *Bias*)则会得到保留,因此高分辨率反演算法无偏是基于尺度转化进行产品验证中的重要条件。TM 反照率与地表测量结果比较的总体偏差不明显。然而,因为数据量的限制以及问题本身的复杂性,本文没有条件对升尺度聚合过程中误差的变化进行更深入的讨论,所以暂时使用误差上限进行估计。

在验证过程中,云对验证精度的干扰很大。云对可见光范围内的辐射反射能力很强,会造成反照率反演值的大幅升高。而云影则会对地面形成阴影,使反照率值反演的偏低。这两种状况都会造成验证数据间的较大偏差。在验证前通过对 TM 影像的判读,筛选无云数据进行验证,有效减少了由云引起的误差。但是在 1 km 或 5 km 范围内仍然会有少量碎云和薄云的存在,碎云和薄云对低分辨率像元尺度的反照率反演和验证的干扰不可以忽略。影响验证误差的另一个重要因素是站点周围地表覆盖的均匀程度。该因素主要影响尺度转换中的精度,不均匀的地表覆盖会增加尺度转换的误差。本文通过选取相对均匀的验证站点来降低这方面的误差。另外,通过对验证数据中绝对误差较大的数据进行详细检查发现,这些数据多为在降雪条件下观测。由于雪地反照率值较高,所以绝对误差偏大,但其相对误差与其他数据接近。

5 结 论

本文利用 FLUXNET 站点数据和 TM 高分辨率反照率对 GLASS 反照率产品进行了验证。TM 高分辨率反照率在反演中采用了 AB 算法,反映出 AB 算法具有以下优势:(1)充分考虑了地表的非朗伯特性并进行了修正;(2)时间分辨率高,时间匹配准确;(3)大气校正模块集成在算法中,不需要大气参数。但是,AB 算法是为低分辨率卫星反照率反演开发的,其训练数据集源自 POLDER-BRDF 数据,该数据的空间分辨率为 6 km,与 TM 影像尺度差异很大,因此在反演 TM 反照率时 AB 算法可能不够稳定。

在 TM 高分辨率反照率经过验证后,本文对其进行聚合以进行尺度转换,但尺度转换的方法较简单,对地形造成的影响考虑不足,可能会增加验证过程中的误差。并且在利用聚合反照率对 GLASS 反照率进行验证时,验证结果中聚合反照率整体偏高于 GLASS 反照率产品,聚合过程中可能存在系统偏差,需要进一步验证确认并分析原因。

通过对结果的分析,本文可得到以下结论:

(1)AB 算法反演的 TM 高分辨率反照率经过 FLUXNET 站点数据的验证,具有较高的精度。

(2)基于尺度转换的验证,GLASS 反照率产品具有较高的精度,能准确反映验证站点的地表反照率及变化趋势。

志 谢 感谢 FLUXNET 数据中心提供的地面验证站点数据下载。感谢美国国家地质勘探局提供的 TM 影像数据下载。感谢 GLASS 项目组各位成员提供 GLASS 产品和技术支持。

参考文献(References)

Cescatti A, Marcolla B, Vannan S K S, Pan J Y, Román M O, Yang X Y, Ciais P, Cook R B, Law B E, Matteucci G, Migliavacca M, Moors E, Richardson A D, Seufert G and Schaaf C B. 2012. Intercomparison of MODIS albedo retrievals and in situ measurements across the global FLUXNET network. Remote Sensing of Environment, 121: 323 – 334 [DOI: 10.1016/j.rse.2012.02.019]

Dickinson R E. 1983. Land surface processes and climate—Surface albedos and energy balance. Advances in Geophysics, 25: 305 – 353

焦子锑, 王锦地, 谢里欧, 张颢, 阎广建, 何立明, 李小文. 2005. 地面和机载多角度观测数据的反照率反演及对 MODIS 反照率产品的初步验证. 遥感学报, 9(1): 64 – 72

Lewis P and Barnsley M J. 1994. Influence of the sky radiance distribution on various formulations of the earth surface albedo // Proceedings of the Colloque International Mesures Physiques et Signatures en Teledetection. Val d'Isere: France: 707 – 716

Liang S L, Fang H L, Chen M Z, Shuey C J, Walthall C, Daughtry C, Morisette J, Schaaf C and Strahler A. 2002. Validating MODIS land surface reflectance and albedo products: methods and preliminary results. Remote Sensing of Environment, 83 (1 – 2): 149 – 162 [DOI: 10.1016/S0034 – 4257(02)00092 – 5]

Liang S L, Stroeve J and Box J E. 2005. Mapping daily snow/ice shortwave broadband albedo from Moderate Resolution Imaging Spectroradiometer (MODIS): the improved direct retrieval algorithm and validation with Greenland in situ measurement. Journal of Geophysical Research: Atmospheres, 110 (D10) [DOI: 10.1029/2004JD005493]

Liu N F, Liu Q, Wang L Z and Wen J G. 2011. A temporal filtering al-

gorithm to reconstruct daily albedo series based on GLASS albedo product // Proceedings of the 2011 IEEE International Geoscience and Remote Sensing Symposium. Vancouver, BC: IEEE: 4227 - 4280 [DOI: 10.1109/IGARSS.2011.6050176]

Mason P. 2005. Implementation plan for the global observing system for climate in support of the UNFCCC. 21st International Conference on Interactive Information Processing Systems (IIPS) for Meteorology, Oceanography, and Hydrology. San Diego, CA, USA.

Qu Y, Liu Q, Liang S, Wang L, Liu N and Liu S. 2012. Direct-estimation algorithm for mapping daily land-surface broadband albedo from MODIS data. IEEE Transactions on Geoscience and Remote Sensing, PP(99): 1 [DOI: 10.1109/TGRS.2013.2245670]

Román M O, Schaaf C B, Woodcock C E, Strahler A H, Yang X Y, B raswell R H, Curtis P S, Davis K J, Dragoni D, Goulden M L, Gu L H, Hollinger D Y, Kolb T E, Meyers T P, Munger J W, Privette J L, Richardson A D, Wilson T B and Wofsy S C. 2009. The MODIS (Collection V005) BRDF/albedo product: assessment of spatial representativeness over forested landscapes. Remote Sensing of Environment, 113(11): 2476 - 2498 [DOI: 10.1016/j.rse.2009.07.009]

Sellers P J, Meeson B W, Hall F G, Asrar G, Murphy R E, Schiffer R A, Bretherton F P, Dickinson R E, Ellingson R G, Field C B, Huemmrich K F, Justice C O, Melack J M, Roulet N T, Schimel D S and Try P D. 1995. Remote sensing of the land surface for studies of global change: Models—algorithms—experiments. Remote Sensing of Environment, 51(1): 3 - 26 [DOI: 10.1016/0034 - 4257(94)00061 - Q]

Stokes G M and Schwartz S E. 1994. The Atmospheric Radiation Measurement (ARM) Program: programmatic background and design of the cloud and radiation test bed. Bulletin of the American Meteorological Society, 75(7): 1201 - 1221 [DOI: 10.1175/1520 - 0477(1994)075 < 1201:TARMPP > 2.0.CO;2]

Susaki J, Yasuoka Y, Kajiwara K, Honda Y and Hara K. 2007. Validation of MODIS albedo products of paddy fields in Japan. IEEE Transactions on Geoscience and Remote Sensing, 45(1): 206 - 217 [DOI: 10.1109/TGRS.2006.882266]

Zhang R H, Tian J, Li Z L, Su H B, Chen S H and Tang X Z. 2010. Principles and methods for the validation of quantitative remote sensing products. Science China Earth Sciences, 53(5): 741 - 751 [DOI: 10.1007/s11430 - 010 - 0021 - 3]